PFG 2012 / 4, 0385–0394
Stuttgart, August 2012

Article

Scientist's Idealism versus User's Realism on Radarsat-2 HR Stereo Capability without GCP: Two Cases over North and Arctic Sites in Canada

Thierry Toutin, Khalid Omari, Enrique Blondel, Ottawa, Daniel Clavet, Sherbrooke & Carla Vanessa Schmitt, Ottawa, Canada

Keywords: Radarsat-2, SAR, high-resolution, radargrammetry, DSM, Canadian Arctic

Summary: Digital surface models (DSMs) are extracted from high-resolution Radarsat-2 (R2) stereo images using our new hybrid radargrammetric modeling without ground control point developed at the Canada Centre for Remote Sensing. They are then evaluated over two Canadian northern and Arctic study sites: the first for the scientific validation and the second in the Arctic (steep relief and glaciated surfaces) for the operational evaluation. For the validation site, the bias and elevation linear errors with 68 percent confidence level (LE68) of R2 stereo-extracted DSM compared to lidar data were computed over bare surfaces: LE68 of 3.7 m and no bias were achieved. For the Arctic study site, a large negative bias of 18–20 m and LE68 of 21–30 m were computed versus ICESat data over and outside ice fields, respectively. In addition LE68 of 15 m with equivalent bias was obtained over ice fields with 0°–5° slopes, which generally occurred in ice fields. The large biases certainly suggest a bias in the R2 stereo-model and thus in the metadata used in our hybrid model computation.

Zusammenfassung: *Der Idealismus des Wissenschaftlers und die Realität des Nutzers hinsichtlich der Möglichkeit von Radarsat-2 zu hochaufgelösten Stereoaufnahmen ohne Passpunkte: Zwei Fallbeispiele für nördliche und arktische Gebiete in Kanada.* Digitale Oberflächenmodelle (DOM), die von hochaufgelösten Radarsat-2 (R2) Stereobildern mit Hilfe eines neuen am Kanadischen Fernerkundungszentrum entwickelten hybriden Radargrammetrie-Modells abgeleitet wurden, welches ohne Passpunkte auskommt, werden anhand von zwei Testgebieten in nördlichen bzw. arktischen Regionen Kanadas evaluiert. Die Evaluierung im ersten Testgebiet dient der wissenschaftlichen Validierung, während jene im arktischen Testgebiet (steiles Gelände, Eis als Untergrund) der Untersuchung operationeller Gesichtspunkte dient. Für die Validierung wurden im Gebiet der systematische Fehler und die linearen Höhenfehler des DOMs aus R2-Daten mit dem DOM aus Laserscanning-Daten auf vegetationslosem Boden verglichen und das 68 % Konfidenzniveau (LE68) bestimmt: LE68 betrug 3.7 m. Ein systematischer Fehler konnte nicht festgestellt werden. Für das arktische Testgebiet ergab sich an bzw. außerhalb von Eisfeldern ein großer negativer systematischer Fehler von 18–20 m und ein Wert des LE68 von 21–30 m im Vergleich zu den Daten von ICESat. Darüber hinaus ergaben sich ein Wert für LE68 von 15 m und ein äquivalenter systematischer Fehler über Eisfeldern, die mit 0°–5° geneigt waren, was eine typische Neigung von Eisfeldern darstellt. Die großen systematischen Fehler legen einen Zusammenhang mit systematischen Fehlern im R2 Stereomodell und somit in den Metadaten, die in unserem hybriden Modell verwendet wurden, nahe.

DOI: 10.1127/1432-8364/2012/0125 1432-8364/12/0125 $ 2.50

1 Introduction

Because Canadian Arctic suffers from poorly-known relief and the surface state of glaciated regions is rapidly evolving due to snowfall, snow transport by wind and/or surface melt, remote sensing data (synthetic aperture radar (SAR) or optical) used to retrieve the topography must be acquired with the shortest possible time interval to maximize their coherence or correlation. This is also important because the flow of the glacier (up to a few metres per day) can bias the topographic measurement during this time interval.

Stereo radargrammetry using SAR data, as developed since 1960's by La Prade (1963), Rosenfield (1968), La Prade & Leonardo (1969), Leberl (1972, 1978) and many other afterwards, can thus be an appropriate solution in Canadian Arctic, even if there was no previous radargrammetric experiment over glacierized region, to the best of our knowledge (Toutin 2011). Because the state-of-the-art of radargrammetry and DSM generation using SAR data can be found in many details in Leberl (1990) and Toutin & Gray (2000), it is thus more important to focus on the winning conditions of stereo-radargrammetry in the challenging conditions of a glacierized region. The multi-date across-track capability is not so problematic due to different SAR advantages specific to ice regions. First, the backscatter of SAR sensors is more dependent on the rugosity or the dielectric component, which enable more radiometric contrast and less depth penetration over ice fields covered with supraglacial debris, rock glaciers, moraines, etc. Second, the SAR sensors are operated in all-weather conditions and not dependent on the solar illumination conditions, which thus cancelled the large shadowed areas with optical data in high latitudes. Third, the convergence of heliosynchronous orbits to North/South poles combined with a large range of look angles (20°–60°) gives thus a strong advantage to drastically reduce the temporal variations to few days between the multi-date stereo-images acquired in the highest latitudes. Last but not least, the new satellite SAR sensors have now high-resolution (HR) capabilities (sub to few metres), and are dedicated toward operational applications.

In summary, the choice of SAR stereo-images should resolve the following issues:

- to have an operational SAR system for acquiring the planned data from shallow look angles at the best season corresponding to the end of the melt season with no snow or little soaked snow and supraglacial debris due to freezing/melt process for soaked ice/snow,
- to reduce temporal resolution and then temporal radiometric changes with the orbit convergence and a larger choice of appropriate look angles (from 35°– 50°),
- to reduce illumination and radiometric differences with images having close look angles,
- to increase the SAR backscatter on ice with shallow look angles due to higher surface roughness with supraglacial debris after the melt season,
- to increase the matching performance and reduce the mismatched areas due to less radiometric variations with small intersection angle, and
- to reduce the SAR depth penetration over the "wet or soaked" 1st-ice layer covered by supraglacial debris with shallow look angles (Dall et al. 2001).

Due to the remote and harsh environments of the Canadian Arctic, the 3D geometric processing of SAR images should require no ground control points (GCPs) collected by users for the operational applications. A new hybrid radargrammetric model (Toutin & Omari 2011) was recently developed for Radarsat-2 (R2) at the Canada Centre for Remote Sensing and thus used for the stereo-modeling and the generation of digital surface models (DSM) without GCP. This hybrid model combine the deterministic Toutin's model (Toutin & Chénier 2009), the rational function model (RFM) empirical model and the Radarsat-2 associated metadata. In order to first evaluate the performance of the stereo-radargrammetric process in a well-controlled research environment (scientist's idealism) and after in an operational environment (user's realism), two Canadian northern and Arctic study sites were used: the first one for the scientific validation and the second one for the operational evaluation in Arctic. This last experiment was the first application of stereo-radargrammetry on glacierized region.

2 Field Study Sites

The first study site (validation site hereafter) is located north of Québec City, Québec, Canada and spans different environments: urban and residential, semi-rural and forested (Fig. 1). The elevation ranges almost from 10 m in the city in the southeast to around 1000 m in the Canadian Shield in the north. The northern part is a hilly to mountainous topography (5°–30° slopes) mainly covered with forests (deciduous, conifer and mixed) while the south part is a semi-flat topography (0°–5° slopes) with urban and residential areas. This site is to validate the quality output products in a well-controlled research environment: the scientist's idealism.

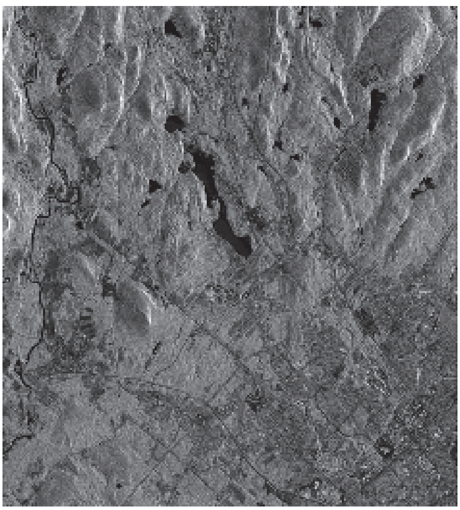

Fig. 1: Radarset-2 (R2) ultra-fine mode (U2) image of the 1st study site. "Radarsat-2 Data ©MacDonald, Dettwiler and Associates Ltd. (2008) – All Rights Reserved" and Courtesy of CSA.

The second study site (operational site hereafter) located in the Baffin Island, Nunavut at approximately 70° 50' N and 71° 30' W (Fig. 2, left). There is no vegetation cover, except small plants. Even if there is some residual snow in the highest altitude on the Landsat ortho-image acquired at the beginning of the melt season in August (Fig. 2, right), the ice fields are similar to the exposed ice surfaces of Jakobshavn Isbrae, west Greenland, where a depth penetration of 1±2 m with C-band radar was found (Rignot et al. 2001). More than 80 % is covered by ice fields with cirque glaciers (permanent ice-covered mountains), outlets and valley glaciers and glaciers tongues surrounded by spectacular fjords with 70°–90° cliffs of 500–800 m height. Bare surface

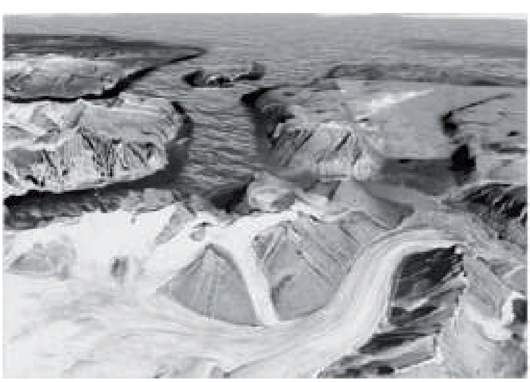

Fig. 2: Left: Perspective view from south to north of the second study site, generated with Google Earth using images from TerraMetrics and WorldView. © 2010 Google and Images ©2010 TerraMetrics and DigitalGlobe. Right: Ortho-rectified Landsat-7 with 1:50,000 map sheet grid. Some residual snow only appears in the highest altitudes at the beginning of the melt season.

mountains also with steep slopes surround the ice fields and glaciers. The valley glacier in the south-east is about 1-km wide with up-to-4° slopes surrounded by 600 m height bare surface and cirque glaciers. The elevation ranges from sea level to 1840 m and the slopes vary from 0°– 90° at fjord cliffs, illustrating a very challenging environment (in terms of land cover and relief). This site is to validate the quality output products in operational mapping environment: the user's realism.

3 Data Acquisition and Processing

For the validation site, the R2 SAR dataset included two stereo images (20 km by 20 km) acquired September 10 and 14, 2008 with the C-band ultra-fine (U) mode (1 by 1 look; 1.6–2.4 m by 3 m resolution) in VV polarization from descending orbits with view angles of 30.8°–32° (U2 Fig. 1) and 47.5°–48.3° (U25) at the near-far edges, respectively.

The reference cartographic data included ground points, mainly road intersections and electrical poles, collected from a differential global positioning system (DGPS) survey in November 2008 with 3-D ground accuracy of 10–20 cm. The collected points were used as independent check points (ICPs) to quantify/validate our new hybrid model accuracy. In addition, DSM (20 km by 20 km, 1 m spacing) were obtained from a first-echoed return lidar survey collected by GPR Consultants in October 2009 (Fig. 3), and covered the full R2 stereo pair. When compared to the previous DGPS, the positioning and altimetric accuracy (1 σ) of the lidar was computed to be better than 0.3 m and 0.1 m, respectively.

For the operational site, the R2 stereo images were acquired in 2009 from descending orbit with the ultra-fine mode (U mode with 3 m resolution) in HH polarization: U12 (Fig. 4) and U26 (20 km by 20 km; 1.6 m by 2.5–3.0 m pixel spacing) on September 28 with 38.83°–39.84° right look angles and September 9, 2009 with 48.12°–48.93° look angles, respectively. This acquisition period corresponded (i) to the end of the melt season and (ii) to -3°/+3° temperature range generating a freezing/melt process during the night/day, respectively. It results, especially with shallow angles that the 1st layer of the exposed "wet" ice fields covered by supraglacial debris and of the remaining soaked snow in the highest altitudes reduced the SAR depth penetration to its minimum (less than 1 m) due to a high water content and dielectric component (Dall et al. 2001, Gray 2011). The radiometry of these stereo data are, however, dominated by the geometric issues due to high relief with no

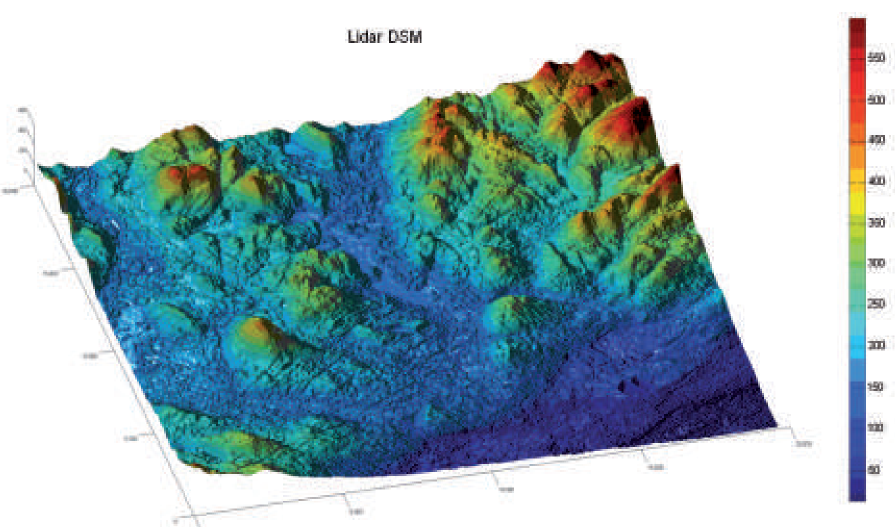

Fig. 3: Digital surface model (20 km by 20 km, 1-m spacing) from a lidar survey.

vegetation cover: more severe layover in U12 over the east-oriented slopes and more occluded areas over the west-oriented slopes in U26. In fact, the south-north curved land-water boundary of the left island represents the cliff layover over the ocean, and not the "smoother" coast line of a glacial-eroded fjord, as well as part of the low lands along this coastline cliff thus "disappeared" due to severe layover. On the other hand, it is almost impossible to discriminate the true water-land boundary for the opposite coastline cliffs due to the SAR shadow/occluded areas.

We can notice on Fig. 2 and Fig. 4 that all coastline cliffs and most cirque glaciers as having strong slopes (60°–90°) while the ice fields with their outlet glaciers have in general lower slopes (0°–20°). However, steep 20°–90° slopes also occurred in some ice fields. The lidar ICESat data (ascending and descending tracks) over the 27F13 map sheet was extracted from GLA14 product (L2 global land surface altimetry data) Release 28, 29 and 31 over the full life cycle of the mission 2003–2008. Conversion to Canadian reference systems was applied to translate ICESat GLAS data into orthometric heights. ICESat data points were spatially filtered: (1) horizontally to remove redundant values within 100-m radius, and (2) vertically within 1-arcsec grid spacing (around 25 m at 70° latitude), to remove potential elevation anomalies resulting from clouds or valley fog.

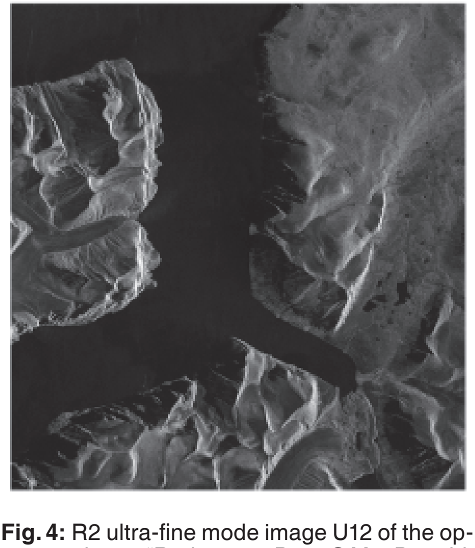

Fig. 4: R2 ultra-fine mode image U12 of the operational site. "Radarsat-2 Data © MacDonald, Dettwiler and Associates Ltd. (2009) – All Rights Reserved" and Courtesy of CSA.

The processing steps for DSM generation with HR SAR stereo-images were previously addressed and documented (Toutin 2010). The new hybrid Toutin's model developed for the radargrammetric processing of R2 at CCRS does not require any GCP collected by the user (Toutin & Omari 2011): it only uses the information in the metadata of the images for computing its parameters. The hybrid model has been proven to be 25-cm precise (Toutin & Chénier 2009), and the accuracy (1 σ) of the results in stereoscopy was better than one pixel with one-pixel biases in the three axes. The main processing steps, which used CCRS scientific software (steps 1–3 & 6) and commercial OrthoEngine^{SE} software of PCI Geomatics[1] (steps 4 & 5), are:

1. Acquisition and pre-processing of the SLC SAR images (speckle filtering with adaptive Frost SAR filter using 11 by 11 window) and metadata;
2. Collection of 60 ICPs from the DGPS survey, only for the validation site;
3. Computation of our hybrid models and their validation with ICPs (systematic and random errors) (Toutin & Omari 2010);
4. Elevation extraction using a 7-step hierarchical grey-level image matching (mean normalized cross-correlation method with sub-pixel computation of the maximum of the correlation coefficient) performed on the quasi-epipolar stereo-images, (Ostrowski & Cheng 2000). Different matching parameterization for both sites were tested to increase the matching success and to reduce elevation interpolation (Toutin 2010);
5. Edition of the quasi-epipolar DSM (blunders removal, gap interpolation, water bodies), and geocoding of the edited quasi-epipolar DSM.
6. Evaluating (systematic and random errors) the geocoded DSMs with the lidar elevation data (Toutin 2010).

[1] In 2012, all steps can be operationally performed within PCI Geomatics.

4 Results and Discussions

Results are related to the systematic and random errors (1) of the hybrid radargrammetric models computed over ICPs and (2) of the stereo-extracted DSMs computed over the lidar elevation data.

4.1 *Radargrammetric Hybrid Model Evaluation*

Because there was no control data in the operational site, Tab. 1 only summarizes the results of the radargrammetric modelling computation for the validation site and dataset previously described: the errors (bias and standard deviation (Std) in metres) computed over 60 DGPS ICPs providing independent and unbiased evaluations of the modelling accuracy. Biases of one pixel (or half SAR resolution) are obtained. Similarly, Std results in the order of one pixel are better for X-direction. It is certainly due to the better knowledge of the range direction than the azimuth direction corresponding to the satellite displacement. Both results in Z-direction are also very good versus the SAR resolution and the same-side stereo geometry. These results are comparable (10 % difference), but a little worse in the Y-direction, to the original radargrammetric model computed with user-collected GCPs (Toutin & Chénier 2009). On the other hand, the small lost in accuracy for the hybrid model is compensated by the gain of processing the stereo images without GCP.

4.2. *DSM Evaluation*

Validation site

Due to the few percents (less than 3 %) of sparse and small mismatched areas (mainly on water bodies), a basic cubic interpolation was performed to fill the gap without introducing significant additional errors. Visually, the DSM in the quasi-epipolar geometry before the geocoding (Fig. 5) is smooth and well describes the macro-topography and the macro linear trends with mountains and valleys, enhancing the structural geological framework in the northwest-southeast direction. The mountains and valleys are generally smooth, being a good representation of a Precambrian geomorphology (smoothed-glacial and eroded topography).

The quantitative evaluation was performed over the coverage of the lidar data and DSM, approximately 20 km by 20 km corresponding to 100 % of the stereo-pair and the elevation differences between the lidar and DSM are given in Tab. 2. However, the results computed over the full lidar/R2 overlap (Tab. 2, All surfaces) do not reflect the true DSM accuracy since other sources in the error budget comes from: (1) the footprint and penetration in the vegetated cover are different for both sensors (SAR and lidar); and (2) the compared stereo SAR and lidar points are not at the same elevation in the vegetated cover (70 % of lidar coverage). These errors are thus reflected in the -1.9 m bias due to more depth penetration of lidar in forested areas and 4.7 m LE68 due to differential depth penetration of lidar depending of tree species and densities. The negative bias is consistent with Z-bias error computed over ICPs (Tab. 1). To have the true elevation accuracy, the error evaluation was thus performed only on surfaces where the lidar and stereo SAR points were at the same ground elevation (Tab. 2, two last lines). The bare surfaces included the bare soils and the impervious areas: in the country (fields, highways, roads) and in the urban parts (streets, private/public parking and gardens, etc.) and are rep-

Tab. 1: Modelling results over 60 DGPS independent check points (ICPs) for the validation site: Bias and standard deviation (Std) in metres.

Bias (m)			Std (m)		
X	Y	Z	X	Y	Z
1.8	2.6	−2.7	0.93	1.33	2.34

Tab. 2: Differences between lidar data and R2 DSM over different surface types: Bias and LE68 in metres.

Surfaces	Bias (m)	LE68 (m)
All surfaces	−1.9	4.7
Bare surfaces	−0.9	3.7
Urban surfaces	−0.5	3.2

resentative of the full terrain relief because they occur not only on low lands and slopes but also in the high lands and slopes (mainly, in the northeast). The urban surfaces included the buildings only and occurred generally on low land and slopes in the south and few villages in the high lands and slopes in the north. No significant difference was noticed inside or outside the urban parts, when the matching was successful: almost no bias and LE68 of 3.7 m and 3.2 m are thus obtained for bare surfaces and urban surfaces, respectively. The

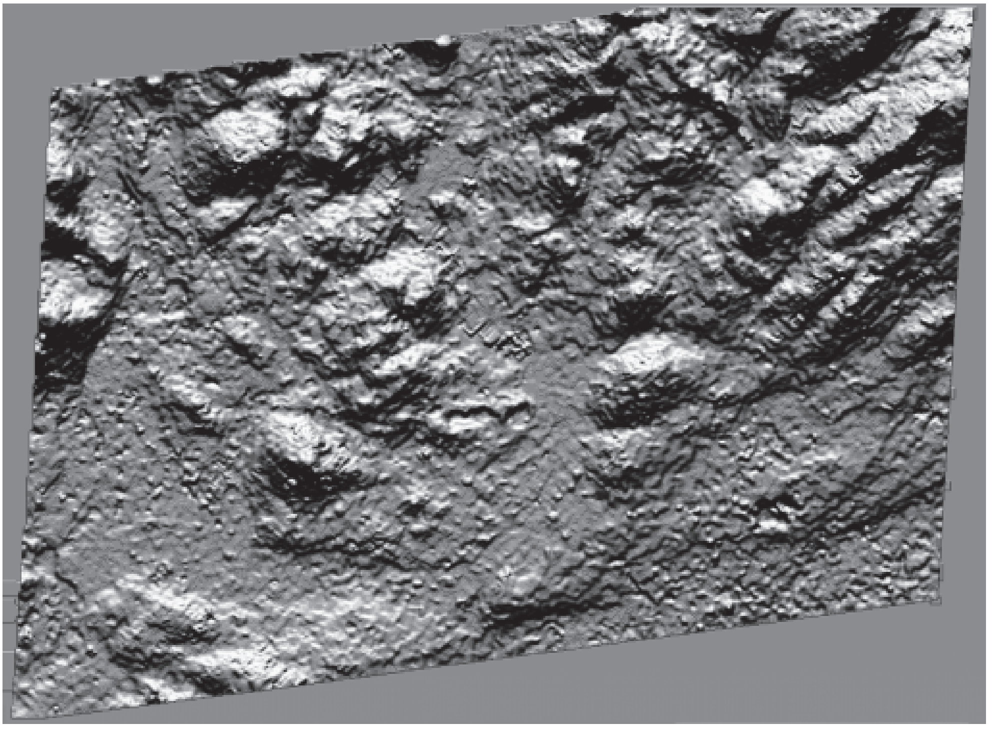

Fig. 5: Shaded-relief DSM (18 km by 16 km) of the validation site in the R2 quasi-epipolar geometry before the geocoding; the main city on low elevations and slopes is in the southeast part.

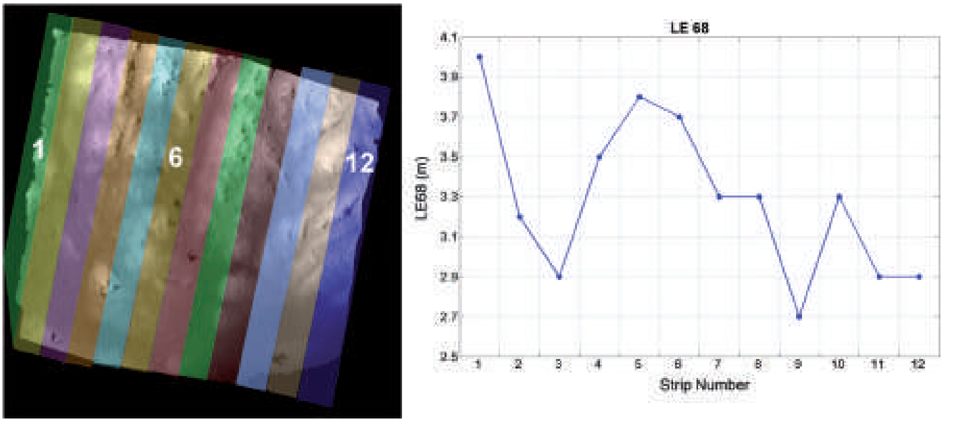

Fig. 6: Left: Geocoded DSM of the validation site with the 12-strip lidar overlaid: Strip 1 at far edge and Strip 12 at near edge. Right: LE68 (in metres) for each strip.

slightly better results over urban surfaces can be due to the fact that most of them generally occurred in low slopes.

The last accuracy evaluation was performed as a function of the SAR range. The lidar data was cut into 12 regular strips (except strip 1), more and less parallel to SAR image azimuth (Fig. 6, left). Strip 1 was at the far edge and strip 12 at the near edge. LE68 (in metres) was thus computed for each strip (Fig. 6, right) and shows there is no correlation between the elevation accuracy and the SAR range, which confirms that the radargrammetric model is not range or look-angle dependent. The result of strip 1 is less significant because there is not enough data when compared to other strips (less than 40 %).

Operational site

The R2 DEM is displayed in Fig. 7 with the ice field and glaciers boundaries (in red) and supraglacial debris and moraines boundaries (in blue). The DEM looks relatively smooth over the ice fields, even with the backscatter homogeneity in ice covered areas, mainly due to the choice of the matching parameterization. In addition, the planned R2 acquisition at the end of the melt season decreased the depth penetration (Dall et al. 2001), increased the roughness and thus the radiometric contrast. During this period, the wet/soaked ice due to freezing/melt process covered by supraglacial debris and dust offered its maximum degree of surface texture and a high backscatter coefficient with shallow SAR look angles. It is the other reason of few percent mismatched areas, which were filled in with the same interpolation without introducing significant additional errors in ice fields. Conversely, the DEM looks very strange along all coast cliffs displaying over 50° slopes and large geometric and radiometric differences between the two images. Instead of generating mismatched pixels, wrong pixels were correlated. The combination of these geometric and radiometric distortions, which only occurred in such a challenging Arctic study site, would certainly impede any image matching system and would have generate either mismatched or wrongly correlated pixels.

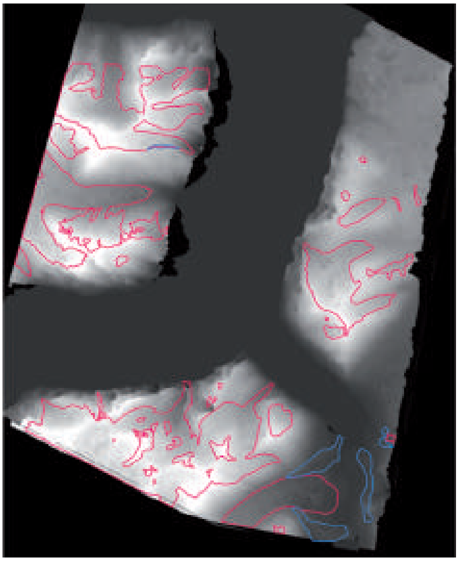

Fig. 7: R2 DSM of the operational site with ice field and glacier boundaries (in red) and supraglacial debris and moraine boundaries (in blue) overlaid.

The quantitative evaluation was performed with ICESat lidar. The height measurements of land surface will be the prime interest for DEM quality assessments (Zwally et al. 2002). While the total number of ICESat data from ascending and descending orbits is limited to thousand points (Fig. 8, blue and red footprints), it will be more limited because ICESat accuracy strongly degrades with slopes. Because the primary goal of ICESat is to measure inter-annual and long-term variations in the polar ice-sheet elevation and volume of Greenland and Antarctica, there were no absolute validation results over more than 5° slopes. Consequently as a function of the expected accuracy for R2 DSM, we only considered for R2 DSM evaluation the ICESat data on slopes less than 30° (Fig. 8, blue footprints). Tab. 3 gives the computed difference between ICESat data and R2 DSM outside (326 points) and over ice fields (387 points).

Because there was no significant bias in the validation site using the same processing, the two biases in this operational site suggest a systematic error in the stereo-model of R2 and thus in the metadata used for this stereo model computation and not from the stereo-radargrammetric processing. While uncertainty about the metadata reliability could

Tab. 3: Differences between ICESat blue footprints and R2 DSM over different surface types: Bias, LE68 and minimum/maximum (Min./Max.) in metres.

Surfaces	ICESat points	Bias (m)	LE68 (m)	Min./Max. (m)
Outside ice fields	326	−16	30	−85/97
Over ice fields	387	−18	21	−88/92

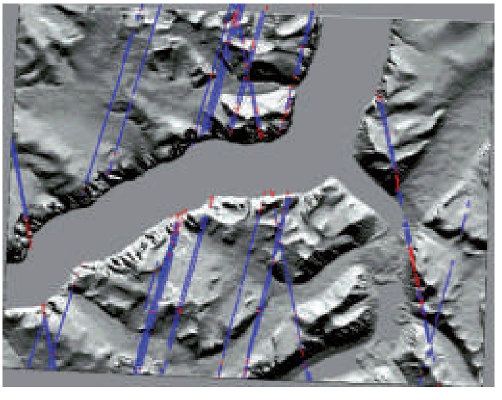

Fig. 8: Ascending and descending ICESat tracks overlaid over a shaded relief image: blue and red footprints are below and over 30° slopes, respectively.

impede the exploitation of the hybrid model with R2 data without GCPs, water bodies or the sea level, frequently occurring in ice regions, can be used for correcting the resulting Z-bias. Because the bias is negatively larger over the ice fields, it is good indication that there was (i) no significant or measurable elevation lowering or ice thinning between the two data acquisitions and (ii) there is no depth penetration. The LE68 over ice fields is a little better (21 m) than outside (30 m) due to less steep slopes over the ice field. In addition, most of ice bodies have low slope relief, other statistical results of elevation differences between ICESat and R2 DEM show that LE68 is strongly correlated with slopes: LE68 of 18 m with an equivalent bias was then computed over ice fields (103 ICESat points) within 0°–5° slopes.

Conclusions

A new hybrid radargrammetric model combining Toutin's deterministic and empirical models and R2 metadata was evaluated with R2 stereo data for DSM generation over two study sites in the north and Arctic of Canada without GCP. The validation site having accurate control data enabled DSM accuracy of 3.7 m (LE68) with no significant bias (-1 m) over bare surfaces to be computed. Even better LE68 (3.2 m) was obtained over buildings, due to their location generally in low slopes. It is certainly the scientist's idealism!

The operational site, a challenging environment with glaciated surfaces, fjords and steep relief, was used to evaluate the mapping potential of the method in the Canadian Arctic without control data. The R2 data acquisition was planned to reduce the SAR depth penetration to its minimum. In this remote and harsh environment, DSM LE68 of 21 m with large bias (-18 m) was achieved over ice field. This major part of this bias is certainly due to a systematic error in the metadata, which can easily be corrected with water bodies or the sea level, which frequently occurred in ice fields. However, the uncertainty of the metadata reliability could slightly impede the operational exploitation of this method due to a possible Z-bias to be corrected: it is maybe the user's realism!

While other methods using optical and SAR systems could achieve similar and even better results, this application demonstrated the capability of R2 to generate DSM with better than 21 m LE68 without collecting control data over ice bodies depending of the terrain slopes (0°–30°) or around 18 m over ice sheets (slopes less than 5°) when the radar penetration is small (less than few metres). This new method increases the applicability of R2 to remote and harsh environments even if there is a slight loss in accuracy when compared to the solution using control points. It is largely compensated by the gain of no control data.

Acknowledgements

The authors would like to thank Paul Briand and the Canadian Space Agency for supporting and financing this research under their SOAR and GRIP programs. They also thank Dr. Philip Cheng and PCI for the adaptation and integration of CCRS math model and algorithms in OrthoEngineSE of PCI Geomatica.

References

Dall, J., Madsen, S.N., Keller, K. & Fosberg, R., 2001: Topography and Penetration of the Greenland Ice Sheet Measured with Airborne SAR Interferometry. – Geophysical Research Letters **28** (09): 1703–1706.

Gray, A.L., 2011: personnel communication.

La Prade, G., 1963: An analytical and experimental study of stereo for radar. – Photogrammetric Engineering **29** (2): 294–300.

La Prade, G. & Leonardo, E., 1969: Elevations from radar imagery. – Photogrammetric Engineering **35** (42): 366–371.

Leberl, F.W., 1972: On model formation with remote sensing imagery. – Österreichische Zeitschrift für Vermessungswesen **2:** 43–61.

Leberl, F.W., 1978: Satellite radargrammetric. – 156 p., Deutsche Geodätische Kommission, Munich, Germany, Serie **C 239**.

Leberl, F.W., 1990: Radargrammetric image processing. – 595 p., Artech House, Norwood, USA.

Ostrowski, J.A. & Cheng, P., 2000: DEM extraction from stereo SAR satellite imagery. – IEEE Geoscience and Remote Sensing Symposium (IGARSS) **2000** (5): 2176–2178, Honolulu, Hawaii.

Rignot, E., Echelmeyer, K. & Krabill, W., 2001: Penetration depth of interferometric synthetic aperture radar signals in snow and ice. – Geophysical Research Letters **28** (18): 3501–3504, doi: 0094-8276/01/2000GL012484.

Rosenfield, G.H., 1968: Stereo radar techniques. – Photogrammetric Engineering **34:** 586–594.

Schwitter, M.P. & Raymond, C.F., 1993: Changes in the Longitudinal Profiles of Glaciers during Advance and Retreat. – Journal of Glaciology **39** (133): 582–590.

Toutin, T., 2000: Elevation Modeling from Satellite Data. – Meyers, R.A. (ed.): Encyclopedia of Analytical Chemistry: 8543–8572, Wiley Publisher.

Toutin, T., 2010: Impact of RADARSAT-2 SAR Ultrafine-Mode Parameters on Stereo-Radargrammetric DEMs. – IEEE Transactions on Geoscience and Remote Sensing **48** (10): 3816–3823.

Toutin, T., 2011: Digital elevation model generation over glacierized regions. – Singh, V.P., Singh, P. & Haritashya, U.K. (eds.): Encyclopedia of Snow, Ice and Glaciers: 202–213, Springer.

Toutin, T. & Chénier, R., 2009: 3-D Radargrammetric Modeling of RADARSAT-2 Ultrafine Mode: Preliminary Results of the Geometric Calibration. – IEEE Geoscience and Remote Sensing Letters **6** (2): 282–286 & **6** (3): 611–615.

Toutin, T. & Gray, A.L., 2000: State-of-the-art of extraction of elevation data using satellite SAR data. – ISPRS Journal of Photogrammetry and Remote Sensing **55** (1): 13–33.

Toutin, T. & Omari, K., 2011: A new hybrid modeling for geometric processing of Radarsat-2 data without user GCP. – Photogrammetric Engineering and Remote Sensing **77** (6): 601–608.

Zwally, H.J., Schutz, B., Abdalati, W., Abshire, J., Bentley, C., Brenner, A., Bufton, J., Dezio, J., Hancock, D., Harding, D., Herring, T., Minster, B., Quinn, K., Palm, S., Spinhirne, J. & Thomas, R., 2002: ICESat's laser measurements of polar ice, atmosphere, ocean, and land. – Journal of Geodynamics **34** (3–4): 405–445.

Addresses of the Authors:

Dr.-Ing. Thierry Toutin, Dr. Khalid Omari & Carla Vanessa Schmitt, Canada Centre for Remote Sensing, Natural Resources Canada, 588 Booth Street, Ottawa, Ontario, K1A 0Y7, Tel.: +1-613-947-1293, -1293, -1326, Fax: +1-613-947-1385, e-mail: {toutin} {komari} {caschmit}@nrcan.gc.ca

Enrique Blondel, Gismatix Inc, 1475 Cumberland Ridge Drive, Ottawa, Ontario, K4C 1E1, Canada, Tel.: +1-613-482-3381, Fax: +1-613-482-3381, e-mail: info@gismatix.ca.

Dr. Daniel Clavet, Centre for Topographic Information, 2144 King Street West, Sherbrooke, Quebec, J1J 2E8, Canada, Tel.: +1-819-564-5600, ext: 255, Fax: +1-819-564-5698, e-mail: dclavet@nrcan.gc.ca

Manuskript eingereicht: Oktober 2011
Angenommen: Februar 2012